Anal Bioanal Chem (2016) 408:6223–6233
DOI 10.1007/s00216-016-9737-z

RESEARCH PAPER

Black phosphorus-assisted laser desorption ionization mass spectrometry for the determination of low-molecular-weight compounds in biofluids

Xiao-Mei He[1] · Jun Ding[1] · Lei Yu[1] · Dilshad Hussain[1] · Yu-Qi Feng[1]

Received: 26 May 2016 / Revised: 15 June 2016 / Accepted: 21 June 2016 / Published online: 6 July 2016

Abstract Quantitative analysis of small molecules by matrix-assisted laser desorption/ionization time-of-flight mass spectrometry (MALDI-TOF MS) has been a challenging task due to matrix-derived interferences in low *m/z* region and poor reproducibility of MS signal response. In this study, we developed an approach by applying black phosphorus (BP) as a matrix-assisted laser desorption ionization (MALDI) matrix for the quantitative analysis of small molecules for the first time. Black phosphorus-assisted laser desorption/ionization mass spectrometry (BP/ALDI-MS) showed clear background and exhibited superior detection sensitivity toward quaternary ammonium compounds compared to carbon-based materials. By combining stable isotope labeling (SIL) strategy with BP/ALDI-MS (SIL-BP/ALDI-MS), a variety of analytes labeled with quaternary ammonium group were sensitively detected. Moreover, the isotope-labeled forms of analytes also served as internal standards, which broadened the analyte coverage of BP/ALDI-MS and improved the reproducibility of MS signals. Based on these advantages, a reliable method for quantitative analysis of aldehydes from complex biological samples (saliva, urine, and serum) was successfully established. Good linearities were obtained for five aldehydes in the range of 0.1–20.0 μM with correlation coefficients (R^2) larger than 0.9928. The LODs were found to be 20 to 100 nM. Reproducibility of the method was obtained with intra-day and inter-day relative standard deviations (RSDs) less than 10.4 %, and the recoveries in saliva samples ranged from 91.4 to 117.1 %. Taken together, the proposed SIL-BP/ALDI-MS strategy has proved to be a reliable tool for quantitative analysis of aldehydes from complex samples.

Keywords Black phosphorus · MALDI matrix · Quaternary ammonium compounds · Stable isotope labeling · Quantitative analysis

Introduction

Matrix-assisted laser desorption/ionization time-of-flight mass spectrometry (MALDI-TOF MS) has been an efficient technique for the analysis of macromolecules, such as peptides, proteins, oligonucleotides, and synthetic polymers [1–3], due to its high throughput, high sensitivity, and low sample consumption. However, quantitative analysis of low molecular weight compounds (<700 Da) by MALDI-TOF MS is still challenging due to the intense background noises derived from the organic matrix and the poor reproducibility of MS signals [4, 5].

To overcome the problem of background interferences in low *m/z* range, several alternative matrices, including organic compounds [6, 7], polymers [8, 9], and inorganic materials [5], have been explored. Among all the newly introduced matrices, inorganic materials, which are usually referred as surface-assisted laser desorption ionization matrices, have gained tremendous attention. Carbon-based materials [10–12], metal/metal oxides [13, 14], and semiconductors [15–17] all exhibited excellent desorption/ionization ability toward various analytes with clear MS backgrounds.

Electronic supplementary material The online version of this article (doi:10.1007/s00216-016-9737-z) contains supplementary material, which is available to authorized users.

✉ Jun Ding
jding@whu.edu.cn

✉ Yu-Qi Feng
yqfeng@whu.edu.cn

[1] Key Laboratory of Analytical Chemistry for Biology and Medicine (Ministry of Education), Department of Chemistry, Wuhan University, Wuhan, Hubei 430072, China

Commonly, a qualified MALDI matrix must fulfill certain criteria including strong UV absorption properties, ability to transfer laser energy to analytes, and few or no matrix background signals [4, 5]. Black phosphorus (BP), the most stable phosphorus allotrope, has been recently recognized as a semiconductor material [18]. After mechanical exfoliation into single- or multi-layer nanosheets, BP showed a layer dependent optical bandgap (ranges from 1.5 eV in monolayer to 0.3 eV in bulk), which covers UV/Vis to infrared regions in electromagnetic spectrum. BP also exhibits relatively higher carrier mobility than some other semiconductor materials such as silicon-based and MoS_2-based devices [19, 20]. Owing to its unique properties, BP has stimulated intense interests in areas of semiconductors [21], electrode materials [22], photoelectric sensors [23], and gas sensors [24]. Moreover, the optical absorption property and high carrier mobility may also endow BP as a promising MALDI matrix candidate. In previous work [25], the feasibility of another phosphorus allotrope, red phosphorus (RP), as MALDI matrix was tested. However, RP was relatively unstable under laser irradiation and generated high phosphorus cluster signals throughout 0–3500 Da region. Thus, the signals of target analytes were illegible in the mass spectra, which restricted RP's application as MALDI matrix. Despite that, the preliminary results on RP did demonstrate the good absorption capacity of phosphorus toward N_2 laser. BP, the most stable of allotrope of phosphorus, could be a promising material to bear laser irradiation and produce less matrix-derived interferences in low *m/z* region. To the best of our knowledge, the application of BP as MALDI matrix has not been exploited so far.

There are several ways to improve the stability of MALDI MS signals, such as increasing the homogeneity of sample/matrix crystallization, introducing internal standards (IS), and data processing through software [3, 26, 27]. Among them, introducing isotopic internal standards before MS analysis is the easiest strategy to adjust the MS signal variations. However, isotopic internal standards are usually expensive or commercially unavailable. In this respect, stable isotope labeling (SIL) strategy, which uses a derivatization reaction to label sample/standard with light/heavy isotope tags followed by mixing the two samples prior to MS analysis, is the best choice to normalize the variation of MS response [28–31]. Moreover, chemical derivatizations are usually used to improve the MS ionization efficiency of analytes [32]. In 2004, a pioneer work which utilized a pair of isotopically coded light/heavy reagents to label amines for MALDI-TOF MS analysis was reported [33]. Although the quantification in this work was only carried out in standard solution, which is probably due to its unsatisfactory performance in complex sample matrix, this work still set a good example to demonstrate the role of SIL strategy in improving both the sensitivity and quantification accuracy of MALDI-TOF MS analysis.

In this work, BP was presented as a MALDI matrix for MALDI-TOF MS analysis of small molecules for the first time. BP is commercially available, and it was directly scribbled onto the MALDI target plate to give a completely even and firm coverage without pre-dispersion processing. As a solvent-free matrix, there were no solvent mixing concerns, maximizing the analytical coverage of analytes and samples. Most interestingly, quaternary ammonium compounds exhibited great sensitivity on MALDI MS using BP as matrix. By combining black phosphorus-assisted laser desorption/ionization mass spectrometry (BP/ALDI-MS) with SIL, sensitive and reliable quantifications of aldehydes from saliva, urine, and serum samples were achieved. The proposed SIL-BP/ALDI-MS strategy has given a comprehensive model that illustrates the performance of MALDI MS for the determination of low-molecular-weight compounds in complex biological samples.

Experimental section

Reagents and materials

Benzo[*a*]pyrene (BaP) was bought from J&K Chemical Ltd. (Tianjin, China). Rhodamine B (RhB), leucomalachite green (LMG), crystal violet (CV), eosin, hexadecyl dimethyl benzyl ammonium chloride (HDBAC), histidine, and aldehyde standards (butanal, hexanal, hepanal, octanal, and nonanal) were purchased from Aladdin Chemical Reagent Co. (Shanghai, China). Sulfhydryl compounds, including *N*-acetyl-cysteine (Nac), glutathione (GSH), cysteine (Cys), and homocysteine (HCys), were purchased from Sigma (St. Louis, MO, USA). Acidic phytohormone standards, IAA, ABA, JA, and SA, were purchased from Olchemim Ltd. (Olomouc, Czech Republic). 4-(2-(Trimethylammonio)ethoxy)-benzenaminium halide (4-APC), d_4-4-(2-(trimethylammonio)ethoxy)-benzenaminium halide (4-APC-d_4), ω-bromoacetonylquinolinium bromide (BQB), and 3-bromoactonyltrimethylammonium bromide (BTA) were synthesized according to our previous works [34–36]. HPLC grade methanol was purchased from TEDIA Co. Inc. (Ohio, USA). Purified water was obtained with a Milli-Q apparatus (Millipore, Bedford, MA, USA). BP, graphene (G), and graphene oxide (GO) were purchased from XFNANO Materials Tech Co. (Nanjing, China), graphite rod was purchased from a local store (Wuhan, China), carbon nanotubes (CNTs) were purchased from Nanotech Port Co. (Shenzhen, China), and fullerene (C60) was purchased from Yongxin Co. (Henan, China).

Characterizations

The microscopic morphology was determined by a Quanta 200 scanning electron microscopy (SEM; FEI, Holland). The element mapping was examined by energy-dispersive

X-ray spectroscopy (EDX) (INCAPentalFETx3, Oxford Instruments). UV/Vis absorption experiment was carried on a Shimadzu UV-2550 spectrometer.

Sample preparation

BP was scribbled onto the MALDI target spot with a diameter approximately 2 mm, then 0.5 μL of analyte solution was pipetted on the top of the matrix layer and dried at ambient conditions followed by MALDI-TOF MS analysis. For comparison, graphite rod was scribbled onto the MALDI target spot; 2 mg mL^{-1} of CNTs, C60, G, and GO solutions were prepared, and 0.5 μL of matrix solution was applied for analysis.

Saliva samples were collected from one nonsmoker and one smoker (up to 10 cigarettes per day). Both saliva samples were collected 2 h after eating. To obtain the saliva samples, each volunteer was told not to swallow the saliva but to store it in their mouths. After 6 min, saliva was collected in Eppendorf tubes and centrifuged at 12,000 g (4 °C) for 5 min. Finally, the supernatant was collected and stored at −80 °C until use.

Human urine and serum samples collected from healthy people were obtained from The Hospital of Wuhan University according to the standard clinical procedures. The utilization of human urine and serum complied with guidelines of Ethics Committee of the Institute, and all participants gave their informed consent. Urine sample collection, pretreatment, and storage were performed according to previous reports [36].

Stable isotope labeling procedure

Labeling of aldehydes by 4-APC

Briefly, 10 μL of $NaBH_3CN$ (1 mg mL^{-1} in methanol) and 20 μL of 4-APC (1 mg mL^{-1} in 50 mM ammonium acetate buffer, pH 5.7) were added to the aldehyde mixture, and the solution was further diluted to 100 μL with 50 mM ammonium acetate buffer (pH 5.7) [36]. After incubation at 25 °C for 1 h with shaking at 1500 rpm, 0.5 μL of the mixed solution was analyzed by MALDI-TOF MS.

For labeling of aldehydes in saliva and serum samples, 20 μL of each sample was diluted to 40 μL with ACN and centrifuged for 5 min at 12,000×*g* (4 °C). The suspensions were further diluted to 100 μL for the derivatization reaction. The process of derivatization is the same as above.

Similar derivatization steps were followed for aldehydes in urine samples, after diluting 10 μL of urine sample to 100 μL for the derivatization reaction.

Labeling of sulfhydryl compounds by BQB

Briefly, 10 μL of BQB (5 mM) was added to the sulfhydryl compound mixture, and the mixed solution was further diluted to 100 μL with Gly–HCl buffer solution (5.0 mM, pH 3.5) [37]. After incubation at 60 °C for 1 h with shaking at 1500 rpm, 0.5 μL of the solution was analyzed by MALDI-TOF MS.

Labeling of acidic phytohormones by BTA

Briefly, 10 μL of triethylamine (TEA; 20 mM) and 10 μL of BTA (20 mM) were added to the acidic phytohormone mixture and further diluted to 100 μL with ACN [35]. Mixture was incubated at 35 °C for 0.5 h by shaking at 1500 rpm, and then 0.5 μL of the solution was analyzed by MALDI-TOF MS.

Mass spectrometry analysis

All MALDI-TOF MS spectra were recorded with an Axima TOF^2 mass spectrometry equipped with a 337-nm nitrogen laser with a 3-ns pulse width (Shimadzu, Kyoto, Japan). The detection was performed in positive ion reflector mode with an accelerating voltage of 20 kV. Typically, 200 laser shots were averaged to generate each spectrum.

Results and discussion

Characterizations

The morphology and element mapping of BP were firstly investigated by SEM and EDX, respectively. A layered structure of commercial bulk BP was observed in SEM image (Fig. 1a). Since the bulk BP is graphite-like, it could be easily scribbled onto the MALDI target spot to make a thin BP layer before analysis. The SEM image of BP layer (Fig. 1b) and its element mapping image of P element (Fig. 1c) showed that BP was evenly distributed on the substrate with a thin layer upon scribbling, which was easy to handle and could improve the shot-to-shot reproducibility during analysis. UV/Vis absorption spectroscopy was used to investigate the optical property of BP layer. Herein, the UV/Vis spectrum of BP was measured on BP solid. As shown in Fig. 1d, a broad absorption band in the UV region (300~350 nm) was observed, indicating the absorption capacity of BP toward N_2 laser (337 nm, a commonly used MALDI laser).

Performance of BP as MALDI matrix

Typically, a good MALDI matrix for small molecule analysis is characterized by two traits: no or few matrix background

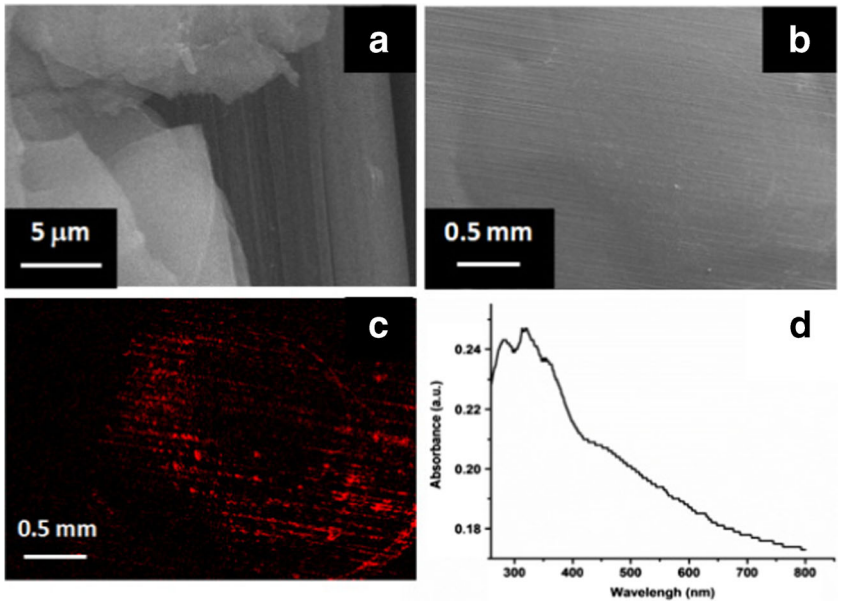

Fig. 1 SEM image of bulk BP (**a**), SEM image of BP scribbled onto the tin foil (**b**), its element mapping image of P element (**c**), and its UV/Vis spectrum (**d**)

ions in the low *m/z* range and good desorption/ionization (*D*/*I*) efficiency toward analytes. To investigate the feasibility of BP as MALDI matrix, the mass spectrum of blank BP in low *m/z* range (0–1000 Da) under the optimal laser intensity (55 %) was recorded. As shown in Fig. 2a, few background interferences were observed, and the existing ion peaks were weak enough (very low signal intensities) to be ignored during analysis, indicating that BP has the potential to be a good MALDI matrix for the analysis of small molecules.

To test BP's *D*/*I* efficiency toward analytes, over 30 kinds of compounds (see Electronic Supplementary Material (ESM) Fig. S1) including acidic compounds (acidic dyes, anionic surfactants, and fatty acid), basic compounds with and without quaternary ammonium cationic group (basic dyes,

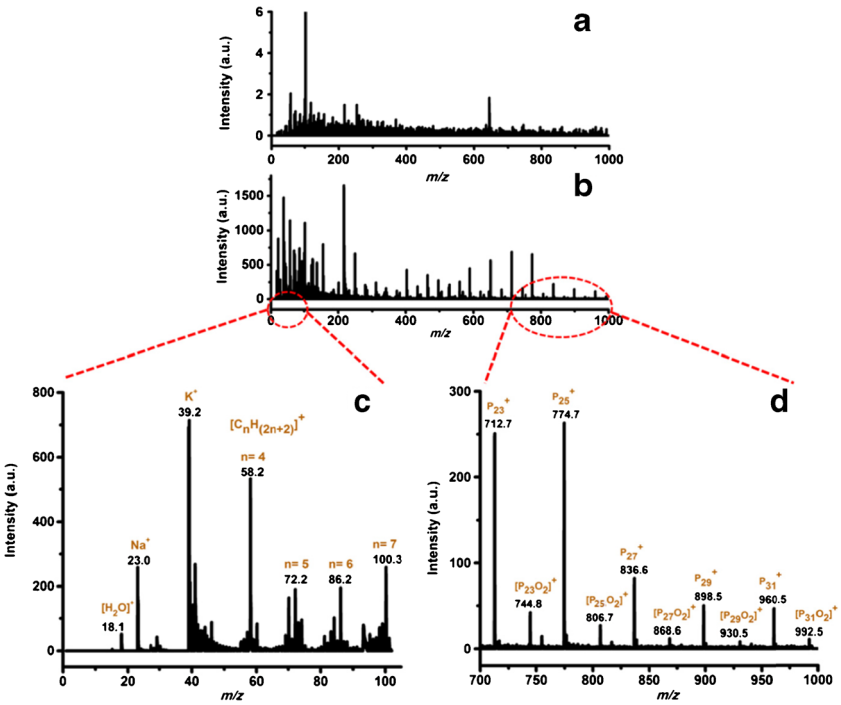

Fig. 2 Mass spectrum of BP matrix with a laser intensity at 55 % (**a**), mass spectrum of BP matrix with a laser intensity at 75 % (**b**), and its enlarge spectra in the *m/z* range of 1–100 (**c**) and 700–1000 (**d**)

antidepressants, and cationic surfactant), amphiprotic compounds (amino acids and peptide), and polyaromatic hydrocarbons were employed as target analytes. It was interesting to note that MS signals of compounds with quaternary ammonium cationic group were strong even at their trace concentration, while signals of other analytes were relatively weak. To find out whether this phenomenon was unique for BP, carbon-based materials including CNTs, C60, graphite, G, and GO were chosen as matrices for comparison. The typical mass spectra of BaP, LMG, and two compounds with quaternary ammonium cationic group (HDBAC and RhB) were recorded with CNTs, graphite, G, GO, C60, and BP as matrices, respectively. BaP and LMG peaks with uneven signal intensities were observed using all six matrices as shown in Fig. 3a, b, and there was no clear advantage in *D*/*I* efficiency of BP compared to carbon-based materials when analyzing BaP and LMG. Moreover, the limits of detection (LODs) for both analytes were up to 0.4 μM. Whereas, in case of compounds with quaternary ammonium cationic group (HDBAC and RhB), MS signals were clearly detected with the assistance of BP, which were accordingly assigned to M^+ (*m/z* at 360.6 and 443.6) of HDBAC and RhB, respectively (Fig. 3c, d). Interestingly, the observed signal intensities of the two positively charged compounds produced by BP were much higher than those obtained by using carbon-based materials, and detection sensitivities improved significantly (LODs at 0.3 and 0.02 nM) further validated the unique superiority of BP as MALDI matrix for compounds with quaternary ammonium cationic group. In addition, HDBAC and RhB could not be easily detected by MALDI MS without the aid of assisted matrix (ESM Fig. S2). To further investigate the unique superiority of BP as MALDI matrix for compounds with quaternary ammonium cationic group, two quaternary ammonium compounds (N^+: CV and RhB) and four non-quaternary ammonium compounds (*X*: histidine, BaP, LMG, and eosin) were mixed together at different mass ratios (N^+: *X* = 1:10, 1:100, and 1:1000) and analyzed using BP as matrix. Figure 4a–c showed that both N^+ could be distinctly detected even at the mass ratio of 1:1000 (Fig. 4c), demonstrating the high sensitivity of BP for N^+ detection. For comparison, CNTs, C60, graphite, G, and GO were also applied for the mixture of N^+ and *X* with a mass ratio at 1:1000. The mass spectra (Fig. 4d–f) showed that, although both N^+ were detected from the mixture using carbon-based matrices, the signal of LMG with a prominent intensity dominated the mass spectra. Furthermore, a histogram illustrating the signal intensity ratios against mass

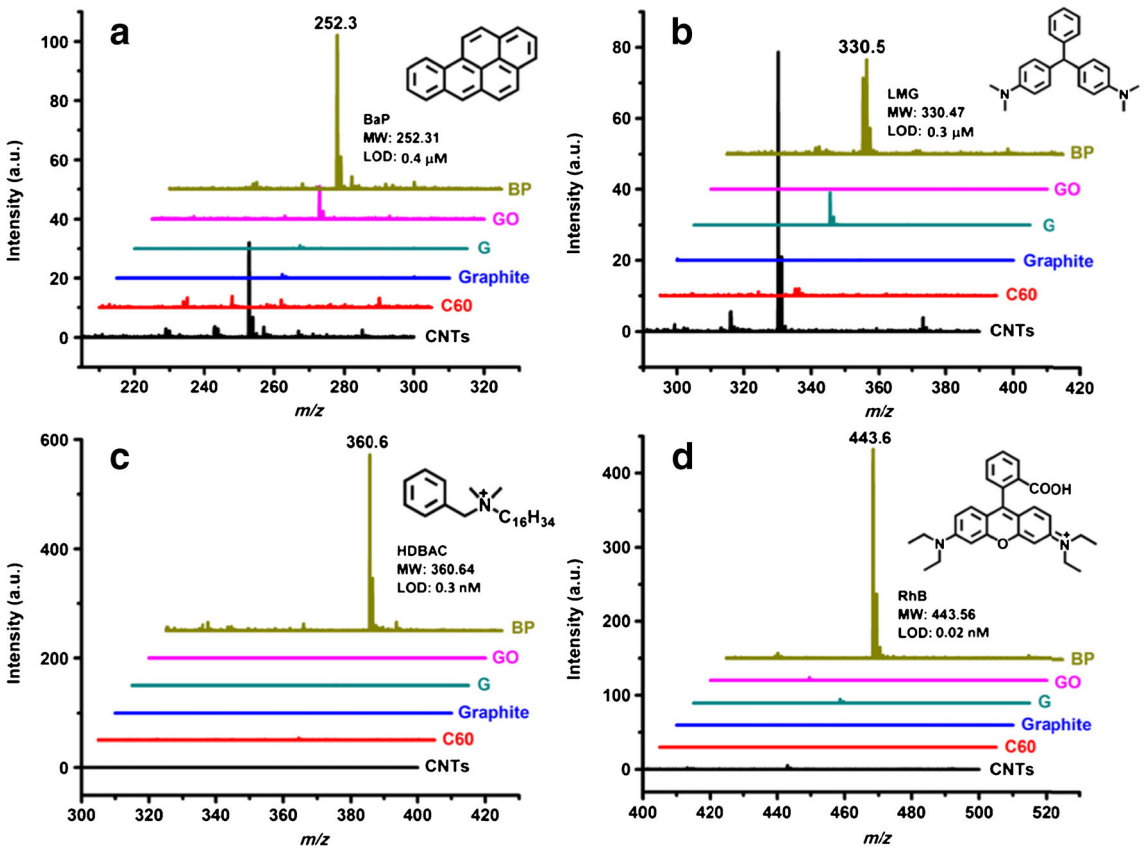

Fig. 3 Mass spectra of (**a**) BaP (4.0 μM), (**b**) LMG (3.0 μM), (**c**) HDBAC (27.8 nM), and (**d**) RhB (2.2 nM) by using CNTs, C60, graphite, G, GO, and BP as the matrices. The inserts were the structural formulas of analytes and their limits of detection (LODs) by BP. Laser intensity, 55 %

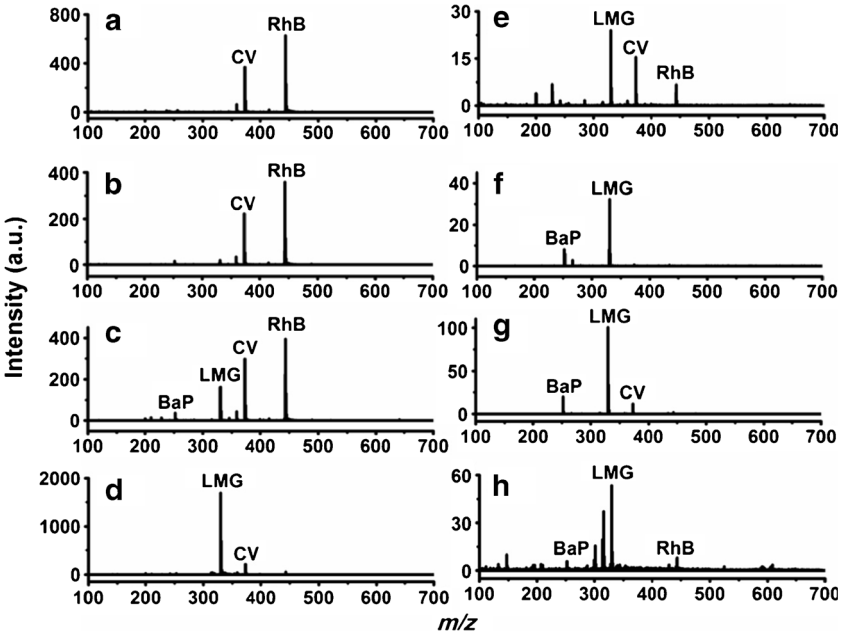

Fig. 4 Mass spectra of the mixtures of quaternary ammonium compounds (N^+) and non-quaternary ammonium compounds (*X*) obtained by BP. Mass ratios of N^+ to *X* were 1:10 (**a**), 1:100 (**b**), and 1: 1000 (**c**). Mass spectra of the mixtures of N^+ and *X* with mass ratio at 1:1000 obtained by CNTs (**d**), C60 (**e**), graphite (**f**), G (**g**), and GO (**h**). The concentration of each N^+ was 10 ng mL^{-1}. The peaks marked with *m/z* were N^+. Laser intensity, 55 %

ratios of N^+ to *X* was also provided to clearly illustrate the sensitivity of BP toward N^+. When the mass ratio of N^+ to *X* was consistent, the intensity ratios of N^+ to *X* obtained from BP were always the highest (ESM Fig. S3). The results indicated that when analyzing cationic compounds in a complicated sample by employing BP as matrix, the signals of cationic compounds might be easy to identify due to good sensitivity of quaternary ammonium compounds on BP.

Salt tolerance of BP was also investigated by detecting RhB (22.6 nM) in 2.0 M NaCl, 2.0 M Tris, and saturated $K_2H_3PO_4$ solution, respectively. The results showed that the signal intensities and signal-to-noise ratio (*S*/*N*) of RhB remained constant and no adduct ions were found in the mass spectra (Fig. 5), demonstrating the high salt tolerance of BP matrix.

BP's amount might have an influence on BP's *D*/*I* efficiency. To investigate the influence of BP's amount on *D*/*I* efficiency, the BP amounts were roughly controlled by increasing the scribbling times of BP on the MALDI target plate from one time to five times. RhB was chosen as a probe, and the signal intensities of RhB with different scribbling times of BP were recorded. Figure S4 in the ESM showed that the signal intensities of RhB almost kept constant with different

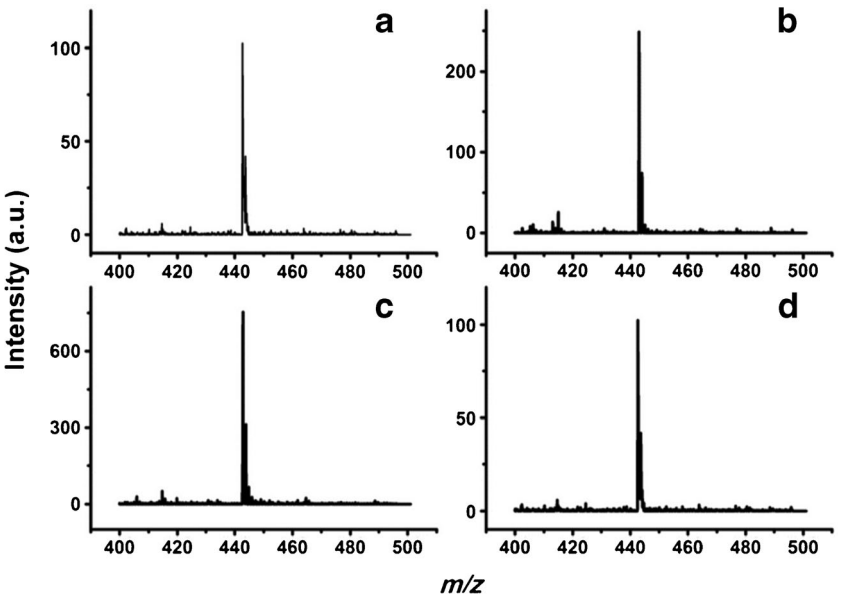

Fig. 5 Mass spectra of RhB (22.5 nM) obtained by BP in the presence of salt: (**a**) without salt, (**b**) 2.0 M NaCl, (**c**) 2.0 M Tris, and (**d**) saturated $K_2H_3PO_4$ solution. Laser intensity, 55 %

scribbling times of BP with a relative standard deviation (RSD) at 4.4 %, indicating that the BP's amount scribbled on the MALDI target plate had minor effect on BP's *D*/*I* efficiency.

Possible mechanism of BP as MALDI matrix

The phenomenon that BP could enhance MALDI MS sensitivity toward quaternary ammonium compounds intrigued us to find out the ionization mechanism underlying the phenomenon. It is well known that the ionization of compounds on MALDI matrix is initiated by the absorption of photons [38]. Since BP has already been demonstrated to offer considerable absorption capability around 300–350 nm (Fig. 1d), which is in accordance with the wavelength of N_2 laser, this property of BP fulfills the preliminary criteria to serve as MALDI matrix. After the absorption of photons, the BP surface might play a critical role in *D*/*I* process. As quaternary ammonium compounds which carry permanent charges do not need the ionization process, the desorption process of quaternary ammonium compounds from assisted matrix is particularly important to the detection sensitivity. To find out what happens to the BP's surface during the desorption process, increasing laser intensity (50–85 %) was used to irradiate the blank BP matrix. Under moderate laser intensity (55 %), a relatively clean spectrum was obtained (Fig. 2a), while at 75 % laser intensity, several abundant peaks with strong intensity could be observed in the mass spectrum (Fig. 2b). In the *m/z* range of 1–100, the *m/z* at 18.1, 23.0, 39.2, and 58.2 were accordingly assigned to $[H_2O]^+$, Na^+, K^+, and adsorbed hydrocarbon contaminants (Fig. 2c), which were also found using some inorganic matrices [16, 38]. In the *m/z* range of 700–1000, a series of regular peaks with mass difference of 62 Da dominated the mass spectrum. For instance, the *m/z* at 712.7, 774.7, 836.6, and 898.5 might be assigned to P_{23}^+, P_{25}^+, P_{27}^+, and P_{29}^+, respectively. And the *m/z* at 744.8 could be $[P_{23}O_2]^+$ because $[PO_2]^+$ was regarded as a charge carrying ion in previous report (Fig. 2d) [39]. The excitation of both small ions (*m/z* at 0–100) and P_n^+ from BP by laser radiation was helpful to release the trapped analytes from the matrix surface into gas phase, which made a great contribution to the desorption process. Besides, these excited ions, including small ions and P_n^+, might be less likely to provide protons to analytes. Therefore, the signal intensities of uncharged compounds remained low, while the signal intensities of compounds with quaternary ammonium cationic group were enhanced. To further explore why BP uniquely exhibited good sensitivity toward the compounds with quaternary ammonium cationic group, the spectra of cluster ions generated from carbon-based materials were also obtained (ESM Fig. S1). Unlike BP, the cluster ions signals of carbon-based materials were less abundant, which might be assigned to relative stability of their inner structure.

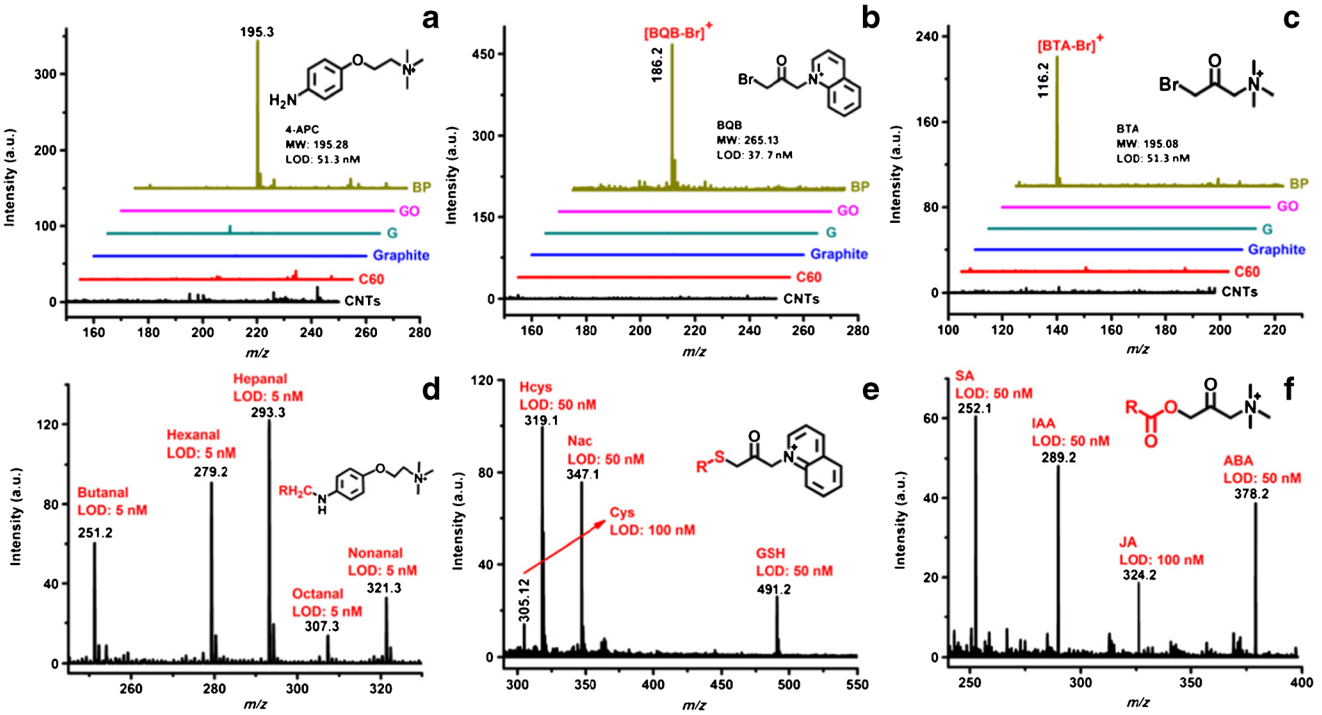

Fig. 6 Mass spectra of (**a**) 4-APC (0.5 μM), (**b**) BQB (0.4 μM), and (**c**) BTA (0.5 μM) by using CNTs, C60, graphite, G, GO, and BP as matrices; mass spectra of (**d**) 4-APC-labeled aldehydes (100 nM), (**e**) BQB-labeled thiols (100 nM), and (**f**) BTA-labeled acidic phytohormones (100 nM) by using BP as matrix. The inserts were the general structural formulas of analytes and their LODs. Laser intensity, 55 %

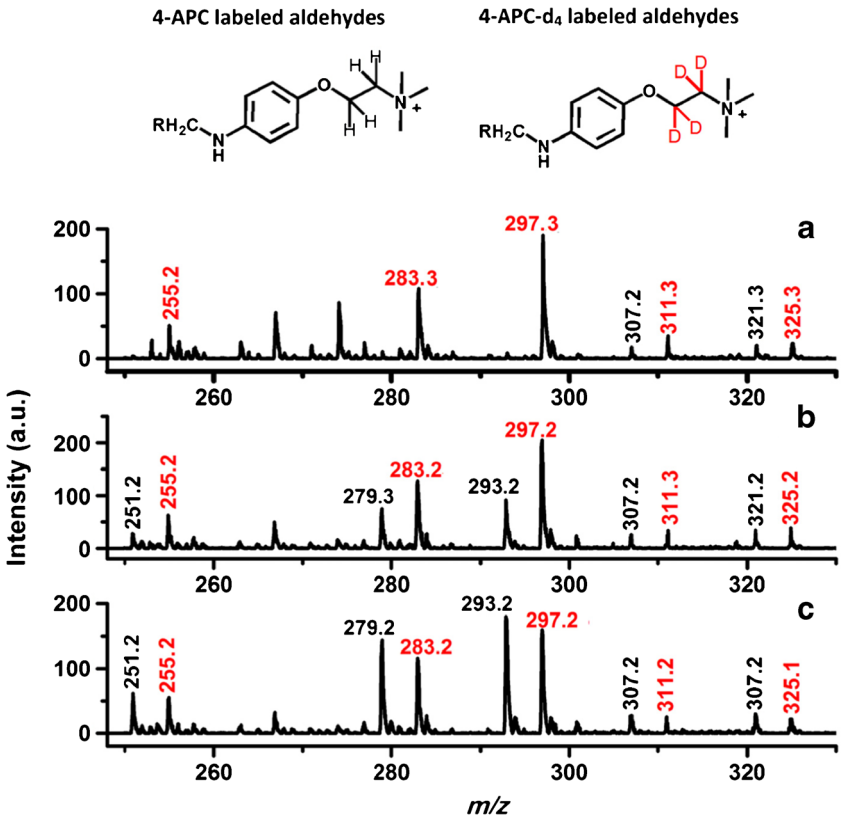

Fig. 7 Mass spectra of 4-APC-labeled saliva samples: (**a**) native saliva, (**b**) saliva spiked with aldehydes (0.5 μM), and (**c**) saliva spiked with aldehydes (1.0 μM). All the saliva samples were spiked with 4-APC-d_4-labeled aldehydes (1.0 μM) as internal standard. Aldehydes: butyraldehyde, hexanal, heptanal, octanal, and nonanal

In this respect, the desorption efficiencies of carbon-based materials were found inferior to BP, resulting in weak sensitivity for detecting the compounds with quaternary ammonium cationic group.

Quantification of small molecules in complex biological samples

The MALDI MS performances of BP implied the potential application of BP in complex biological analysis. However, the superiority of BP toward quaternary ammonium compounds might restrict its universality and practicability. To circumvent the problem, chemical derivatizations were introduced by labeling quaternary ammonium moiety to compounds with different structures. In our previous studies, a series of reagents containing quaternary ammonium groups were synthesized, including 4-APC, BQB, and BTA, which could selectively label quaternary ammonium groups onto aldehydes [36], thiols [37, 40], and carboxyl acids [34, 35], respectively. Mass spectra of these reagents were shown in Fig. 6a–c, target peaks of these reagents could be seen clearly when using BP as matrix, while the signal intensities of the reagents were too weak in the case of the carbon-based materials. The LODs of these reagents obtained by using BP matrix

Table 1 Calibration curves, LODs, and LOQs of five aldehydes in saliva samples

Analytes	Linearity and sensitivity characteristics				
	Linear range (μM)	Regression data ($n = 3$)		LOD (nM)	LOQ (nM)
		Linear equation	R^2 value		
Butyraldehyde	0.5–20	$Y = (0.021 \pm 0.038) + (0.952 \pm 0.032)X$	0.9946	50	165
Hexanal	0.1–20	$Y = (-0.116 \pm 0.030) + 1.089 \pm 0.038)X$	0.9928	20	66
Heptanal	0.1–20	$Y = (-0.062 \pm 0.013) + (1.102 \pm 0.036)X$	0.9946	20	66
Octanal	0.5–20	$Y = (-0.032 \pm 0.061) + (0.863 \pm 0.020)X$	0.9974	100	330
Nonanal	0.5–20	$Y = (0.030 \pm 0.041) + (0.909 \pm 0.021)X$	0.9973	100	330

Table 2 Accuracy and precision (intra- and inter-day) for the determination of aldehydes in saliva

Analyte	Intra-day precision (RSD, %, $n = 3$)			Inter-day precision (RSD, %, $n = 3$)			Recovery (%, $n = 3$)		
	Low (1 μM)	Medium (5 μM)	High (10 μM)	Low (1 μM)	Medium (5 μM)	High (10 μM)	Low (1 μM)	Medium (5 μM)	High (10 μM)
Butyraldehyde	2.3	7.0	6.8	13.7	11.1	5.6	104.6 ± 5.9	91.4 ± 4.6	95.9 ± 5.9
Hexanal	4.4	6.0	5.9	5.3	5.4	0.3	107.0 ± 4.6	92.7 ± 6.8	102.7 ± 1.6
Heptanal	1.7	2.3	1.3	5.0	9.5	6.3	96.1 ± 5.4	88.2 ± 5.8	98.2 ± 2.5
Octanal	6.7	7.2	5.9	8.9	0.3	4.0	117.1 ± 7.4	105.3 ± 3.8	96.8 ± 4.3
Nonanal	10.4	5.4	6.0	11.2	10.3	5.9	105.4 ± 8.6	103.6 ± 5.9	101.5 ± 4.8

were less than 51.3 nM. After chemical derivatization with these reagents, the detection sensitivities of aldehydes, thiols, and acid derivatives were significantly improved by using BP as matrix (LODs at 5~100 nM) (Fig. 6d–f). These results demonstrated the introduction of chemical derivatization strategy contributed to both the improved coverage of analytes as well as the detection sensitivity.

We further evaluated the efficiency of BP matrix for quantitative analysis of analytes in real biological samples by MALDI MS. To obtain a reliable quantification results, the poor reproducibility of the analyte signals must be improved [41]. SIL strategy was introduced to solve the problem of instability of MS signal in this work. As a proof-of-concept application, SIL was combined with BP-assisted laser desorption/ionization mass spectrometry for quantification of aldehydes in saliva, which are considered as the potential biomarkers for oxidative stress and cancer [42]. We used a pair of stable isotope probes, 4-APC and 4-APC-d_4, to label five kinds of aldehydes in saliva samples and standard aldehydes, respectively. After labeling, the mass difference between 4-APC- and 4-APC-d_4-labeled aldehydes imparted by SIL strategy was 4 Da, and the 4-APC-d_4-labeled standards were employed as internal standards for MALDI MS signal correction. The linearities were conducted by analyzing saliva samples spiked with fixed amount of 4-APC-d_4-labeled aldehydes (1.0 μM) and 4-APC-labeled aldehyde at concentrations of 0.1, 0.5, 1, 2, 5, 10, and 20 μM, respectively. As shown in typical mass spectra of 4-APC-labeled aldehydes and 4-APC-d_4-labeled aldehydes in saliva samples (Fig. 7), the signal intensity ratios (light/heavy) increased linearly with the increase of the spiking concentrations of 4-APC-labeled aldehydes, indicating that the signal intensity ratios closely matched with the molar ratios of different isotope-labeled compounds; thus, the MS signal variation was corrected. Specifically, satisfactory calibration curves were obtained by plotting signal intensity ratios (analyte/IS) versus concentrations of 4-APC-labeled aldehydes with correlation coefficients (R^2) ranging from 0.9928 to 0.9974 for five aldehydes in saliva (Table 1). The limits of detection (LODs) and the limits of quantification (LOQs), defined as the amounts of the analytes at an *S*/*N* of 3 and 10, respectively, were in the range of 20–100 and 66–330 nM, respectively.

The accuracy and precision of the developed method were assessed by the recoveries and the intra- and inter-day RSDs. Both recoveries and intra- and inter-day RSDs were calculated with aldehydes standards spiked in saliva samples at three concentration levels (1, 5, and 10 μM). For each concentration, triplicate measurements were performed. Intra-day variation was evaluated by repeating the analysis for three times within 1 day, and the inter-day variation was investigated on three successive days. The relative recoveries were calculated by comparing the calculated concentration of spiked aldehydes in the saliva samples to the actual spiked concentration. As shown in Table 2, acceptable precision was achieved with RSD values less than 10.4 %, and the relative recoveries were in the range of 88.2–117.1 %, indicating good reproducibility and accuracy of the developed method.

In real sample analysis, aldehydes in saliva samples from one nonsmoker and one smoker were determined using the proposed method, and both samples were analyzed in triplicates. It was found that the aldehyde contents in smoker saliva were higher than that of nonsmoker (Table 3).

Encouraged by the good performance obtained from saliva samples, we further applied the method in more complex samples like urine and serum samples (see ESM Table S1 and Figs. S6 and S7). As a result, urinary heptanal from a pooled urine sample could be detected but not quantitative, and the

Table 3 Endogenous contents of aldehydes in saliva samples

Analytes	Detected contents (μM, RSD%, $n = 3$)	
	Nonsmoker	Smoker
Butyraldehyde	NQ	0.10 (4.6)
Hexanal	NQ	3.36 (12.2)
Heptanal	NQ	0.87 (5.8)
Octanal	0.77 (10.8)	3.00 (13.5)
Nonanal	1.06 (5.3)	6.86 (5.6)

NQ not quantified

content of heptanal in the pooled serum sample was 0.40 μM (RSD = 3.8 %, $n = 3$). The aforementioned results indicated that SIL-BP/ALDI-MS is a feasible tool for the quantification of small molecules from complex biological fluids.

Conclusion

In this, BP was successfully used as MALDI matrix for the analysis of small molecules. The proposed BP/ALDI-MS showed higher detection sensitivity for quaternary ammonium compounds with considerable salt tolerance. By combining BP/ALDI-MS with SIL strategy, the analyte coverage was expanded and a variety of compounds, including aldehydes, thiols, and carboxyl acids, were detected after derivatization with labeling reagents containing quaternary ammonium moiety; signal variation of MALDI MS was corrected, thus aldehydes in biological fluids were accurately determined. The proposed approach exhibited strong ability in the quantitative analysis of aldehydes in complex samples including saliva, urine, and serum. We believe that this work presents a promising strategy for small molecules analysis using MALDI-TOF MS.

Acknowledgments We are thankful for the financial support from the National Basic Research Program of China (973 Program) (2013CB910702), the National Natural Science Foundation of China (21475098), and the Fundamental Research Funds for the Central Universities.

Compliance with ethical standards

Conflict of interest The authors declare that they have no conflict of interest.

Ethical consent Human urine and serum samples collected from healthy people were obtained from The Hospital of Wuhan University according to the standard clinical procedures. The utilization of human urine and serum complied with guidelines of Ethics Committee of the Institute, and all participants gave their informed consent.

References

1. Domon B, Aebersold R. Mass spectrometry and protein analysis. Science. 2006;312:212–7.
2. Tsao CW, Yang ZJ. High sensitivity and high detection specificity of gold-nanoparticle-grafted nanostructured silicon mass spectrometry for glucose analysis. ACS Appl Mater Interfaces. 2015;7(40):22630–7.
3. Wei YB, Li SM, Wang JX, Shu CY, Liu JA, Xiong SX, et al. Polystyrene spheres-assisted matrix-assisted laser desorption ionization mass spectrometry for quantitative analysis of plasma lysophosphatidylcholines. Anal Chem. 2013;85(9):4729–34.
4. Guinan T, Kirkbride P, Pigou PE, Ronci M, Kobus H, Voelcker NH. Surface-assisted laser desorption ionization mass spectrometry techniques for application in forensics. Mass Spectrom Rev. 2015;34(6):627–40.
5. Law KP, Larkin JR. Recent advances in SALDI-MS techniques and their chemical and bioanalytical applications. Anal Bioanal Chem. 2010;399(8):2597–622.
6. Chen SM, Chen L, Wang JN, Hou J, He Q, Liu JA, et al. 2,3,4,5-Tetrakis(3′,4′-dihydroxylphenyl)thiophene: a new matrix for the selective analysis of low molecular weight amines and direct determination of creatinine in urine by MALDI-TOF MS. Anal Chem. 2012;84(23):10291–7.
7. Ayorinde FO, Hambright P, Porter TN, Keith QL. Use of mesotetrakis(pentafluorophenyl)porphyrin as a matrix for low molecular weight alkylphenol ethoxylates in laser desorption/ionization time-of-flight mass spectrometry. Rapid Commun Mass Spectrom. 1999;13(24):2474–9.
8. Woldegiorgis A, Kieseritzky F, Dahlstedt E, Hellberg J, Brinck T, Roeraade J. Polymer-assisted laser desorption/ionization analysis of small molecular weight compounds. Rapid Commun Mass Spectrom. 2004;18(8):841–52.
9. Hua L, Low TY, Meng W, Chan-Park MB, Sze SK. Novel polymer composite to eliminate background matrix ions in matrix assisted laser desorption/ionization-mass spectrometry. Analyst. 2007;132(12):1223–30.
10. Dong XL, Cheng JS, Li JH, Wang YS. Graphene as a novel matrix for the analysis of small molecules by MALDI-TOF MS. Anal Chem. 2010;82(14):6208–14.
11. Hopwood FG, Michalak L, Alderdice DS, Fisher KJ, Willett GD. C60-assisted laser desorption/ionization mass spectrometry in the analysis of phosphotungstic acid. Rapid Commun Mass Spectrom. 1994;8(11):881–5.
12. Xu SY, Li YF, Zou HF, Qiu JS, Guo Z, Guo BC. Carbon nanotubes as assisted matrix for laser desorption/ionization time-of-flight mass spectrometry. Anal Chem. 2003;75(22):6191–5.
13. McLean JA, Stumpo KA, Russell DH. Size-selected (2−10 nm) gold nanoparticles for matrix assisted laser desorption ionization of peptides. J Am Chem Soc. 2005;127(15):5304–5.
14. Lorkiewicz P, Yappert MC. Titania microparticles and nanoparticles as matrixes for in vitro and in situ analysis of small molecules by MALDI-MS. Anal Chem. 2009;81(16):6596–603.
15. Lin Z, Zheng J, Lin G, Tang Z, Yang X, Cai Z. Negative ion laser desorption/ionization time-of-flight mass spectrometric analysis of small molecules using graphitic carbon nitride nanosheet matrix. Anal Chem. 2015;87(15):8005–12.
16. Wei J, Buriak JM, Siuzdak G. Desorption-ionization mass spectrometry on porous silicon. Nature. 1999;399(6733):243–6.
17. Go EP, Apon JV, Luo GH, Saghatelian A, Daniels RH, Sahi V, et al. Desorption/ionization on silicon nanowires. Anal Chem. 2005;77(6):1641–6.
18. Kou L, Chen C, Smith SC. Phosphorene: fabrication, properties, and applications. J Phys Chem Lett. 2015;6(14):2794–805.
19. Zhang X, Xie H, Liu Z, Tan C, Luo Z, Li H, et al. Black phosphorus quantum dots. Angew Chem Int Edit. 2015;54(12):3653–7.
20. Li L, Yu Y, Ye GJ, Ge Q, Ou X, Wu H, et al. Black phosphorus field-effect transistors. Nat Nanotechnol. 2014;9(5):372–7.
21. Liu H, Neal AT, Zhu Z, Luo Z, Xu XF, Tománek D, et al. Phosphorene: an unexplored 2D semiconductor with a high hole mobility. ACS Nano. 2014;8(4):4033–41.
22. Sun LQ, Li MJ, Sun K, Yu SH, Wang RS, Xie HM. Electrochemical activity of black phosphorus as an anode material for lithium-ion batteries. J Phys Chem C. 2012;116(28):14772–9.
23. Dai J, Zeng XC. Bilayer phosphorene: effect of stacking order on bandgap and its potential applications in thin-film solar cells. J Phys Chem Lett. 2014;5(7):1289–93.
24. Kou LZ, Frauenheim T, Chen CF. Phosphorene as a superior gas sensor: selective adsorption and distinct I–V response. J Phys Chem Lett. 2014;5(15):2675–81.

25. Liu ZY, Huang RB, Zheng LS. Bare phosphorus and binary phosphide cluster ions generated by laser ablation. Z Phys D: At, Mol Clusters. 1996;38(2):171–7.
26. He XM, Zhu GT, Yin J, Zhao Q, Yuan BF, Feng YQ. Electrospun polystyrene/oxidized carbon nanotubes film as both sorbent for thin film microextraction and matrix for matrix-assisted laser desorption/ionization time-of-flight mass spectrometry. J Chromatogr A. 2014;1351:29–36.
27. Liland KH, Mevik BH, Rukke EO, Almoy T, Isaksson T. Quantitative whole spectrum analysis with MALDI-TOF MS, part II: determining the concentration of milk in mixtures. Chemometr Intell Lab. 2009;99(1):39–48.
28. Guo K, Li L. Differential C-12/C-13-isotope dansylation labeling and fast liquid chromatography/mass spectrometry for absolute and relative quantification of the metabolome. Anal Chem. 2009;81(10):3919–32.
29. Bruheim P, Kvitvang HFN, Villas-Boas SG. Stable isotope coded derivatizing reagents as internal standards in metabolite profiling. J Chromatogr A. 2013;1296:196–203.
30. Huang YQ, Wang QY, Liu JQ, Hao YH, Yuan BF, Feng YQ. Isotope labelling—paired homologous double neutral loss scan-mass spectrometry for profiling of metabolites with a carboxyl group. Analyst. 2014;139(13):3446–54.
31. Hsu JL, Huang SY, Chow NH, Chen SH. Stable-isotope dimethyl labeling for quantitative proteomics. Anal Chem. 2003;75(24):6843–52.
32. Qi BL, Liu P, Wang QY, Cai WJ, Yuan BF, Feng YQ. Derivatization for liquid chromatography-mass spectrometry. TrAC Trends Anal Chem. 2014;59:121–32.
33. Lee PJ, Chen W, Gebler JC. Qualitative and quantitative analysis of small amine molecules by MALDI-TOF mass spectrometry through charge derivatization. Anal Chem. 2004;76(16):4888–93.
34. Huang YQ, Liu JQ, Gong HY, Yang J, Li YS, Feng YQ. Use of isotope mass probes for metabolic analysis of the jasmonate biosynthetic pathway. Analyst. 2011;136(7):1515–22.
35. Chen ML, Huang YQ, Liu JQ, Yuan BF, Feng YQ. Highly sensitive profiling assay of acidic plant hormones using a novel mass probe by capillary electrophoresis-time of flight-mass spectrometry. J Chromatogr B. 2011;879(13–14):938–44.
36. Yu L, Liu P, Wang YL, Yu QW, Yuan BF, Feng YQ. Profiling of aldehyde-containing compounds by stable isotope labelling-assisted mass spectrometry analysis. Analyst. 2015;140(15):5276–86.
37. Huang YQ, Ruan GD, Liu JQ, Gao Q, Feng YQ. Use of isotope differential derivatization for simultaneous determination of thiols and oxidized thiols by liquid chromatography tandem mass spectrometry. Anal Biochem. 2011;416(2):159–66.
38. Chen SM, Zheng HZ, Wang JN, Hou J, He Q, Liu HH, Xiong CQ, Kong XL, Nie ZX. Carbon nanodots as a matrix for the analysis of low-molecular-weight molecules in both positive- and negative-ion matrix-assisted laser desorption/ionization time-of-flight mass spectrometry and quantification of glucose and uric acid in real samples. Anal Chem. 2013:6646-6652.
39. Martin TP. Compound clusters. Z Phys D: At, Mol Clusters. 1986;3(2):211–7.
40. Liu P, Huang YQ, Cai WJ, Yuan BF, Feng YQ. Profiling of thiol-containing compounds by stable isotope labeling double precursor ion scan mass spectrometry. Anal Chem. 2014;86(19):9765–73.
41. van Kampen JJA, Burgers PC, de Groot R, Gruters RA, Luider TM. Biomedical application of MALDI mass spectrometry for small-molecule analysis. Mass Spectrom Rev. 2011;30(1):101–20.
42. Hasnis E, Reznick AZ, Pollack S, Klein Y, Nagler RM. Synergistic effect of cigarette smoke and saliva on lymphocytes—the mediatory role of volatile aldehydes and redox active iron and the possible implications for oral cancer. Int J Biochem Cell B. 2004;36(5):826–39.